J. Fluid Mech. (2011), *vol.* 679, *pp.* 544–558.
doi:10.1017/jfm.2011.144

The effect of viscous dissipation on the onset of convection in an inclined porous layer

D. A. NIELD[1], A. BARLETTA[2]† AND M. CELLI[2]

[1]Department of Engineering Science, University of Auckland, Private Bag 92019, Auckland 1142, New Zealand

[2]DIENCA, Alma Mater Studiorum – Università di Bologna, Viale Risorgimento 2, Bologna 40136, Italy

(Received 24 October 2010; revised 19 March 2011; accepted 20 March 2011; first published online 18 May 2011)

The linear stability of a basic forced and free convection flow in an inclined porous channel is analysed by using the Darcy law and the Oberbeck–Boussinesq approximation. The basic velocity and temperature distributions are influenced by the effect of viscous dissipation, as well as by the boundary conditions. The boundary planes are assumed to be impermeable and isothermal, with a temperature of the lower boundary higher than that of the upper boundary. The instability against longitudinal rolls is studied by employing a second-order weighted residual solution and an accurate sixth-order Runge–Kutta solution of the disturbance equations. The instability against transverse rolls is also investigated. It is shown that these disturbances are in every case less unstable than the longitudinal rolls.

Key words: buoyancy-driven instability, convection in porous media, porous media

1. Introduction

The onset of flow instability, induced by the viscous dissipation effect, has been the subject of several investigations carried out through the last decades. Joseph (1965) studied the thermal instability of plane Couette flow and of Poiseuille flow in a circular pipe due to the non-uniform thermal gradient caused by viscous dissipation in the fluid. Along those lines, further developments were carried out by Sukanek, Goldstein & Laurence (1973), who obtained neutral stability curves for plane Couette flow with different values of the Brinkman number, and by Cheng & Wu (1976), who analysed the linear stability of Poiseuille flow in a plane channel with isothermal walls and heated from below. Ho, Denn & Anshus (1977) extended the linear stability analysis of plane Couette flow developed by Sukanek *et al.* (1973), adopting an accurate numerical integration of the coupled equations for the velocity and temperature disturbances, and also studying the case of Poiseuille flow in a circular pipe. More recently, these stability problems were revisited by Yueh & Weng (1996), Johns & Narayanan (1997) and Subrahmaniam, Johns & Narayanan (2002). Some authors also considered the thermal instability induced by viscous dissipation in plane Couette flow, or in plane Couette–Poiseuille flow, with reference to non-Newtonian fluids (Eldabe, El-Sabbagh & El-Sayed (Hajjaj)

† Email address for correspondence: antonio.barletta@unibo.it

2007; Nouar & Frigaard 2009). We mention that all the papers cited above are theoretical investigations of thermal instability in a basic shear flow where the velocity–temperature coupling is due to a temperature-dependent viscosity. On the other hand, the buoyancy effect is neglected.

The role played by the buoyancy force in the onset of convective instability is a challenging subject when the basic state of the fluid displays an unstable thermal stratification caused by internal viscous dissipation, and not by an externally imposed bottom heating as in the classical Rayleigh–Bénard problem. Recently, there has been an increase in interest in the effect of viscous dissipation in convection both in porous media and in fluids clear of solid material. In particular, viscous dissipation effects on the onset of convection in a porous medium have been studied by Barletta, Celli & Rees (2009*a*, *b*), Barletta, Celli & Nield (2010), Nield & Barletta (2009, 2010), Storesletten & Barletta (2009) and Barletta & Nield (2010). The last authors treated the case of Hadley–Prats flow (the extension of the well-known Horton–Rogers–Lapwood problem to the case of horizontal throughflow and an inclined temperature gradient), a situation for which the basic flow is one-dimensional. Closely related to the Hadley flow problem is the problem of convection in an inclined porous layer. The latter problem has been studied by several people, notably Weber (1975), Caltagirone & Bories (1986) and Rees & Bassom (2000), and further literature on the subject has been reviewed by Nield & Bejan (2006) and Nield (2011). Again the basic flow is one-dimensional, and Weber (1975) was able to deduce, under the assumption of a small inclination angle, some stability results for the inclined layer problem from those for the Hadley problem.

In this paper, we extend the results on flow stability in an inclined porous layer by including the effects of a basic mass flow rate in the layer and of the viscous dissipation associated with this basic flow. Due to the effect of the viscous dissipation, the basic flow is no longer given by a simple linear polynomial expression and, in order to obtain it, one has to solve a nonlinear ordinary differential equation. However, an approximate polynomial solution for the basic flow, valid for the realistic assumption of a very small Gebhart number, is considered here in developing the linear stability analysis.

We finally mention that a very interesting experimental work on the effect of viscous dissipation for the flow instability was recently carried out by White & Muller (2002). These authors refer to Taylor–Couette flow and investigate the onset of the instability due to the coupling of viscous heating and centrifugal destabilization in glycerin–water solutions and in a polybutene oligomer.

2. Mathematical model

We consider a layer of a saturated porous medium inclined at an angle ϕ to the horizontal, confined between the planes $\overline{z}=0$ and $\overline{z}=H$, with the $\overline{x}$-axis in the direction up the plane. Each boundary plane is impervious. The plane $\overline{z}=0$ is held at temperature $\overline{T}=T_0+\Delta T$ and the plane $\overline{z}=H$ is held at temperature T_0 (see figure 1). All the overlined quantities refer to dimensional variables.

Let us assume that

(i) Darcy's law holds;
(ii) the Oberbeck–Boussinesq approximation can be applied;
(iii) the viscous dissipation cannot be neglected;
(iv) a condition of local thermal equilibrium holds.

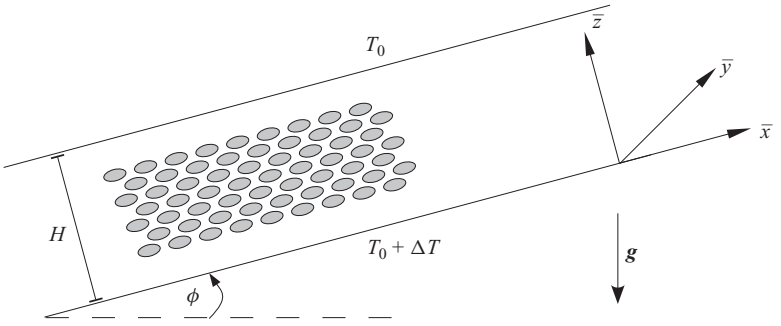

FIGURE 1. A sketch of the porous layer.

Then, the governing balance equations can be written as

$$\overline{\nabla}\cdot\overline{\boldsymbol{u}} = 0, \tag{2.1}$$

$$\frac{\mu}{K}\overline{\boldsymbol{u}} = -\overline{\nabla}\overline{p} + \rho_f\, g\, \beta\, \overline{T}(\sin\phi\, \boldsymbol{e}_1 + \cos\phi\, \boldsymbol{e}_3), \tag{2.2}$$

$$(\rho\, c)_m \frac{\partial \overline{T}}{\partial \overline{t}} + (\rho\, c)_f\, \overline{\boldsymbol{u}}\cdot\overline{\nabla}\ \overline{T} = k_m \overline{\nabla}^2 \overline{T} + \frac{\mu}{K}\,\overline{\boldsymbol{u}}\cdot\overline{\boldsymbol{u}}, \tag{2.3}$$

where $\overline{\boldsymbol{u}}$ is the Darcy velocity, while ρ, β and μ denote the density, volumetric coefficient of thermal expansion and dynamic viscosity, respectively, while g is the modulus of the gravitational acceleration, K is the permeability of the porous medium, c denotes the specific heat and $\boldsymbol{e}_1$, $\boldsymbol{e}_2$, $\boldsymbol{e}_3$ are the unit vectors in the $\overline{x}$, $\overline{y}$, $\overline{z}$ directions. The term $(\rho c)_m$ is the heat capacity per unit volume of the porous medium, $(\rho c)_f$ is the heat capacity per unit volume of the fluid and k_m is the effective thermal conductivity of the porous medium. In particular, ρ_f is the fluid density at temperature T_0.

The boundary conditions are given by

$$\overline{z} = 0\colon \quad \overline{w} = 0, \quad \overline{T} = T_0 + \Delta T, \tag{2.4}$$

$$\overline{z} = H\colon \quad \overline{w} = 0, \quad \overline{T} = T_0. \tag{2.5}$$

2.1. *Dimensionless formulation*

Let us introduce the scaling

$$\overline{\boldsymbol{x}} = \boldsymbol{x}\, H, \quad \overline{t} = t\, \frac{\sigma\, H^2}{\alpha}, \quad \overline{\boldsymbol{u}} = \boldsymbol{u}\, \frac{\alpha}{H}, \quad \overline{p} = p\, \frac{\alpha\, \mu}{K}, \quad \overline{T} = T_0 + T\, \Delta T, \tag{2.6}$$

where α is the thermal diffusivity and σ is the heat capacity ratio:

$$\alpha = \frac{k_m}{(\rho\, c)_f}, \quad \sigma = \frac{(\rho\, c)_m}{(\rho\, c)_f}. \tag{2.7}$$

Equations (2.1)–(2.3) then take the dimensionless form

$$\nabla\cdot\boldsymbol{u} = 0, \tag{2.8}$$

$$\boldsymbol{u} = -\nabla\, p + R\, T\, (\sin\phi\, \boldsymbol{e}_1 + \cos\phi\, \boldsymbol{e}_3), \tag{2.9}$$

$$\frac{\partial T}{\partial t} + \boldsymbol{u}\cdot\nabla T = \nabla^2 T + \frac{Ge}{R}\,\boldsymbol{u}\cdot\boldsymbol{u}, \tag{2.10}$$

where the Darcy–Rayleigh number R and the Gebhart number Ge are defined by

$$R = \frac{\rho_f \, g \, \beta \, K \, H \Delta T}{\mu \, \alpha}, \quad Ge = \frac{\beta \, g \, H}{c_f}. \tag{2.11}$$

Equations (2.8)–(2.10) are to be solved subject to the boundary conditions

$$z = 0 : \qquad w = 0, \quad T = 1, \tag{2.12}$$

$$z = 1 : \qquad w = 0, \quad T = 0. \tag{2.13}$$

One can eliminate the pressure by taking the curl of (2.9). This gives

$$\nabla \times \boldsymbol{u} = R \, \nabla \times [T \, (\sin \phi \, \boldsymbol{e}_1 + \cos \phi \, \boldsymbol{e}_3)]. \tag{2.14}$$

3. Basic solution

We assume a basic flow with a purely transverse temperature gradient. We now seek a basic steady-state solution of the form

$$u = u_B(z), \quad v = w = 0, \quad T = T_B(z), \tag{3.1}$$

where the subscript 'B' stands for 'basic flow'. Equations (2.10) and (2.14) give

$$\frac{\mathrm{d}^2 T_B}{\mathrm{d}z^2} + \frac{Ge}{R} \, [u_B(z)]^2 = 0, \tag{3.2}$$

$$\frac{\mathrm{d}u_B}{\mathrm{d}z} = R \, \frac{\mathrm{d}T_B}{\mathrm{d}z} \, \sin \phi. \tag{3.3}$$

The last equation integrates to give

$$u_B = R \, \sin \phi \, (T_B + C), \tag{3.4}$$

where C is a constant. Substitution in (3.2) then gives the nonlinear equation

$$\frac{\mathrm{d}^2 T_B}{\mathrm{d}z^2} + Ge \, R \, (T_B + C)^2 \, \sin^2 \phi = 0. \tag{3.5}$$

Equation (3.5) is to be solved subject to the boundary conditions

$$T_B(0) = 1, \quad T_B(1) = 0, \tag{3.6}$$

and to the constraint

$$\int_0^1 u_B \, \mathrm{d}z = \int_0^1 R \, \sin \phi \, (T_B + C) \, \mathrm{d}z = Pe, \tag{3.7}$$

where Pe is the Péclet number associated with the basic flow. The constant C is thus expressed as

$$C = \frac{Pe}{R \, \sin \phi} - \int_0^1 T_B \, \mathrm{d}z. \tag{3.8}$$

One can now define the parameter Λ as

$$\Lambda = Ge \, Pe^2. \tag{3.9}$$

We note that usually the Gebhart number is extremely small. For instance, if $H = 0.1$ m and we consider dry air at 300 K, then $\beta = 1/300 \, \mathrm{K}^{-1}$ and $c_f = 10^3 \, \mathrm{J \, kg^{-1} \, K^{-1}}$. This means, on account of (2.11), that $Ge \cong 3 \times 10^{-6}$. On the other hand, the Péclet

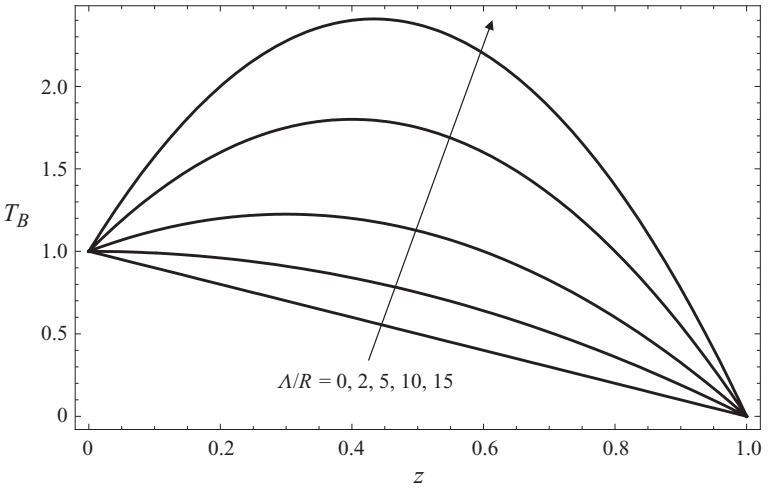

FIGURE 2. Plots of the basic temperature profile $T_B(z)$ for different values of Λ/R.

number can be very large especially when highly viscous fluids are considered. Thus, it is physically reasonable to assume $Ge \ll 1$, $Pe \gg 1$ so that $\Lambda \sim O(1)$ and $R \sim O(1)$ (see, for instance, Barletta, Celli & Rees 2009*a*, *b*). Under these hypotheses, one can conclude that $Ge\,Pe \ll 1$ and $Ge\,R \ll 1$. One can thus apply a regular perturbation procedure to obtain the approximate solution as a function of the parameter $\gamma = Ge\,R\,\sin^2\phi \ll 1$. We look for a T_B expressed as

$$T_B = T_{B,0} + \gamma\, T_{B,1} + O(\gamma^2). \tag{3.10}$$

The basic temperature and velocity profiles at $O(\gamma)$ can be written as

$$T_B \approx 1 - z + \frac{\gamma}{12}\left[\frac{1}{16} - \left(z - \frac{1}{2}\right)^4\right] + \frac{z\,Ge\,Pe\,\sin\phi}{6}\left[1 + \frac{3\,Pe}{R\,\sin\phi} - 3z\left(1 + \frac{Pe}{R\,\sin\phi}\right) + 2z^2\right], \tag{3.11}$$

$$u_B \approx R\,\sin\phi\left(T_B - \frac{1}{2}\right) + Pe. \tag{3.12}$$

Taking into account that $\Lambda \sim O(1)$, $Ge\,Pe \ll 1$ and $Ge\,R \ll 1$, one can simplify (3.11) and (3.12) by keeping only the dominant terms

$$T_B \approx (1 - z)\left(1 + z\,\frac{\Lambda}{2\,R}\right), \tag{3.13}$$

$$u_B \approx R\,\sin\phi\left[(1 - z)\left(1 + z\,\frac{\Lambda}{2\,R}\right) - \frac{1}{2}\right] + Pe. \tag{3.14}$$

Plots of the basic temperature profiles are shown in figure 2. The basic profile is potentially unstable for every value of the parameter Λ/R because, on the lower boundary $z = 0$, a temperature higher than that on the upper boundary $z = 1$ is prescribed. On the other hand, for increasing values of Λ, thus for a stronger contribution of the viscous heating, the basic temperature profile shows increasing values of the average temperature.

When γ is not small, one can still obtain an analytical solution involving an incomplete elliptic integral of the first kind (Abramowitz & Stegun 1965). In the remainder of this paper, just the case of small γ is considered. Given the very small values assumed by Ge, this limit appears in fact as the only physically sensible regime.

3.1. *The inclined channel and the Hadley–Prats flow*

We mentioned that Weber (1975), by considering small inclination angles, proposed a solution of the stability problem for an inclined channel with isothermal walls by developing an analogy with the Hadley problem. One could consider the possibility that such an analogy can be extended for the case with a net mass flow rate ($Pe \neq 0$) and with non-negligible viscous dissipation. This possibility appears to be out of reach for the following reason. The net mass flow rate in an inclined channel may influence the temperature distribution only through the effect of viscous dissipation, whereas the net mass flow rate in the Hadley–Prats flow may influence the temperature distribution even with negligible viscous dissipation (Barletta & Nield 2010). In other words, in the inclined channel, when $Ge \to 0$ (negligible viscous dissipation) the basic temperature distribution is not influenced by Pe. This conclusion is easily drawn from (3.5) and (3.6). The Hadley–Prats problem, examined by Barletta & Nield (2010), is different as the basic temperature distribution in the layer depends on Pe even when the viscous dissipation is negligible ($Ge \to 0$). This important difference in the physics of the Hadley–Prats problem, with respect to the inclined channel problem, is the reason why the approximation of small-Ge adopted here ($Ge \ll 1$, $Pe \gg 1$ so that $\Lambda \sim O(1)$), could not be consistently applied in the analysis of the Hadley–Prats flow (Barletta & Nield 2010).

4. Linear disturbances

We perturb the basic solution by setting

$$u = u_B + \varepsilon\, U, \quad v = \varepsilon\, V, \quad w = w_B + \varepsilon\, W, \quad T = T_B + \varepsilon\, \theta, \tag{4.1}$$

where ε is a small parameter. On substituting (4.1) in (2.8), (2.10) and (2.14) and neglecting the nonlinear terms $O(\varepsilon^2)$, we obtain the linearized stability equations, namely

$$\nabla \cdot \boldsymbol{U} = 0, \tag{4.2}$$

$$\nabla \times \boldsymbol{U} = \nabla \times [R\,\theta\,(\sin\phi\,\boldsymbol{e}_1 + \cos\phi\,\boldsymbol{e}_3)], \tag{4.3}$$

$$\frac{\partial \theta}{\partial t} + u_B\,\frac{\partial \theta}{\partial x} + W\,\frac{\mathrm{d}T_B}{\mathrm{d}z} = \nabla^2\theta + 2\,\frac{Ge}{R}\,u_B\,U. \tag{4.4}$$

Here, $\boldsymbol{U}$ denotes the vector (U, V, W). Consistently with the approximation $Ge \ll 1$, $Pe \gg 1$, so that $\Lambda \sim O(1)$ and $R \sim O(1)$, the last term on the right-hand side of (4.4) can be neglected. In fact, as a consequence of (3.14), this term is of order $Ge\,Pe$. One can thus simplify (4.4) as follows:

$$\frac{\partial \theta}{\partial t} + u_B\,\frac{\partial \theta}{\partial x} + W\,G(z) = \nabla^2\theta, \tag{4.5}$$

where $G(z)$ is defined as

$$G(z) = \frac{\mathrm{d}T_B}{\mathrm{d}z} = (1 - 2\,z)\,\frac{\Lambda}{2\,R} - 1. \tag{4.6}$$

From (2.12) and (2.13), the boundary conditions are given by

$$z = 0, 1: \qquad W = \theta = 0. \tag{4.7}$$

In this paper, we consider an inclined porous layer without any lateral confinement. In the absence of viscous dissipation, it is well known that the most unstable linear disturbances are longitudinal rolls (see, for instance, Rees & Bassom 2000), i.e. wave-like disturbances invariant along the x direction. We will first assume, in the following section, that the viscous dissipation effect is not so strong as to alter this pattern selection for the instability. Then, we will illustrate how the action of transverse rolls, i.e. wave-like disturbances invariant along the y direction, implies higher values of the critical Rayleigh number for the onset of the instability than the action of longitudinal rolls.

5. Longitudinal rolls

Assuming the disturbances to be x-independent longitudinal rolls, the solutions of (4.2), (4.3), (4.5) and (4.7) are thus sought such that $U = 0$ and the fields V, W, θ depend only on (y, z, t). It is now convenient to introduce a streamfunction, ψ, such that (4.2) is satisfied,

$$V = \frac{\partial \psi}{\partial z}, \quad W = -\frac{\partial \psi}{\partial y}. \tag{5.1}$$

Equations (4.3) and (4.5) can thus be rewritten as

$$\nabla^2 \psi = -R \frac{\partial \theta}{\partial y} \cos\phi, \tag{5.2}$$

$$\frac{\partial \theta}{\partial t} - \frac{\partial \psi}{\partial y} G(z) = \nabla^2 \theta. \tag{5.3}$$

We seek solutions of the disturbance equations for the analysis of stability in the form of plane waves,

$$\psi(y, z, t) = \mathrm{Re}\left\{i\, f(z)\, \mathrm{e}^{\mathrm{i}(a y - \lambda t)}\right\}, \quad \theta(y, z, t) = \mathrm{Re}\left\{h(z)\, \mathrm{e}^{\mathrm{i}(a y - \lambda t)}\right\}, \tag{5.4}$$

where Re denotes the real part of a complex function, a is the real wavenumber, $\lambda = \lambda_R + \mathrm{i}\,\lambda_I$ is a complex exponent, and $f(z)$ and $h(z)$ are the complex disturbance amplitudes. When $\lambda_I > 0$, the disturbance is growing exponentially and that means instability, whereas $\lambda_I < 0$ implies an exponentially damped disturbance and that means stability. Because we are interested in the threshold condition of neutral stability, we now set $\lambda_I = 0$, so that

$$f'' - a^2 f + a\, R \cos\phi\; h = 0, \tag{5.5}$$

$$h'' - (a^2 - \mathrm{i}\,\lambda_R)\; h - a\, G(z)\, f = 0, \tag{5.6}$$

where $\lambda_R = \mathrm{Re}\{\lambda\}$ and the primes denote differentiation with respect to z. The eigenvalue problem becomes self-adjoint assuming $\lambda_R = 0$. Now if one rescales the amplitude h as

$$\widetilde{h} = h\, R \cos\phi, \tag{5.7}$$

the system of (5.5)–(5.6) becomes

$$f'' - a^2 f + a\, \widetilde{h} = 0, \tag{5.8}$$

$$\widetilde{h}'' - a^2\, \widetilde{h} - a\, \widetilde{G}(z)\, f = 0, \tag{5.9}$$

where

$$\widetilde{G}(z) = G(z)\, R\, \cos\phi = (1 - 2\,z)\,\frac{\widetilde{\Lambda}}{2} - \widetilde{R}, \quad \widetilde{\Lambda} = \Lambda\, \cos\phi, \quad \widetilde{R} = R\, \cos\phi. \tag{5.10}$$

The system thus rescaled loses dependence on the angle ϕ. The boundary conditions can be expressed as

$$z = 0, 1: \qquad f = \widetilde{h} = 0. \tag{5.11}$$

5.1. *A weighted-residuals solution*

An approximate solution of the eigenvalue problem constituted by (5.8)–(5.9) can be obtained by using the Galerkin method of weighted residuals (Finlayson 1972). We denote the trial functions (satisfying the boundary conditions) as f_n, with $n \in \mathbb{N}$, and write

$$f = \sum_{n=1}^{N} A_n\, f_n, \quad \widetilde{h} = \sum_{n=1}^{N} B_n\, f_n. \tag{5.12}$$

In the present case, by taking into account the boundary conditions (5.11), we can choose

$$f_n(z) = \sin(n\,\pi\, z). \tag{5.13}$$

We take $N = 2$, thus obtaining two solutions for $\widetilde{R}$:

$$\widetilde{R} = \frac{18\,a^4\,\pi^2 + 90\,a^2\,\pi^4 + 153\,\pi^6 - \sqrt{729\,\pi^8\left(2\,a^2 + 5\,\pi^2\right)^2 + 1024\,a^4\,\widetilde{\Lambda}^2}}{18\,a^2\,\pi^2}, \tag{5.14}$$

$$\widetilde{R} = \frac{18\,a^4\,\pi^2 + 90\,a^2\,\pi^4 + 153\,\pi^6 + \sqrt{729\,\pi^8\left(2\,a^2 + 5\,\pi^2\right)^2 + 1024\,a^4\,\widetilde{\Lambda}^2}}{18\,a^2\,\pi^2}. \tag{5.15}$$

With respect to (5.14)–(5.15), we will consider the lowest neutral stability curve described by (5.14). We note that, when $\widetilde{\Lambda} = 0$, (5.14) and (5.15), respectively, simplify to

$$\widetilde{R} = \frac{\left(a^2 + \pi^2\right)^2}{a^2}, \tag{5.16}$$

$$\widetilde{R} = \frac{\left(a^2 + 4\,\pi^2\right)^2}{a^2}. \tag{5.17}$$

Equations (5.16) and (5.17) are the well-known relationships for the first two modes of neutral stability in the Horton–Rogers–Lapwood problem.

5.2. *The numerical solution*

The eigenvalue problem defined by (5.8) and (5.9), as well as by (5.11), is here solved numerically by means of a sixth-order Runge–Kutta method coupled with the shooting method. In order to use the Runge–Kutta method, we imposed two additional initial conditions in $z = 0$, namely

$$f'(0) = 1, \quad \widetilde{h}'(0) = \eta, \tag{5.18}$$

where the condition $f'(0) = 1$ fixes the otherwise indeterminate scale of the eigenfunctions $(f, \widetilde{h})$ in (5.8)–(5.9) and the parameter η can be determined by the shooting method. The approximate analytical solution obtained in the preceding section with the method of weighted residuals provides in fact excellent estimates for

$\widetilde{\Lambda}$	$\widetilde{R}_{cr}$	a_{cr}
0	$4\pi^2$	π
100	37.88950	3.232423
200	32.86951	3.516578
300	23.91902	3.954144
400	11.09960	4.399537
471.3847	0	4.675189
500	−4.823007	4.775561
600	−23.06281	5.090010

TABLE 1. Longitudinal rolls: values of $\widetilde{R}_{cr}$ and a_{cr} versus $\widetilde{\Lambda}$.

initializing the Runge–Kutta method. For any given value of the parameter $\widetilde{\Lambda}$, one obtains a functional relationship, $\widetilde{R} = \widetilde{R}(a)$, between the modified Darcy–Rayleigh number, defined in (5.10), and the wavenumber. In particular, on differentiating the system of differential equations (5.8) and (5.9) with respect to a with $\mathrm{d}\widetilde{R}(a)/\mathrm{d}a = 0$, one can obtain two additional differential equations that, together with (5.8) and (5.9), allow one to determine directly the minimum of the function $\widetilde{R}(a)$, i.e. the critical pair $(a_{cr}, \widetilde{R}_{cr})$ for the onset of the convective instability. The sixth-order Runge–Kutta method with an adaptive step-size control is implemented by using the Mathematica 7.0 package (© Wolfram Research, Inc.) and, in particular, by means of the function `NDSolve`. The same software package also allows the implementation of the shooting method by employing the function `FindRoot`. Details about the functions `NDSolve` and `FindRoot` are available in Wolfram (2003).

5.3. *Onset of the instability*

By employing the numerical method illustrated in the preceding section, we were able to obtain the critical values $(a_{cr}, \widetilde{R}_{cr})$ for prescribed values of $\widetilde{\Lambda}$. The parametrization adopted in (5.7)–(5.11) yields a unique pair $(a_{cr}, \widetilde{R}_{cr})$ for a given $\widetilde{\Lambda}$ without any need to prescribe the value of ϕ. In fact, the dependence on the inclination angle remains hidden in the definitions of $(\widetilde{h}, \widetilde{R}_{cr}, \widetilde{\Lambda})$. In this sense, the solution does not distinguish the case of a horizontal channel from that of an inclined channel. Values of $(a_{cr}, \widetilde{R}_{cr})$ are reported in table 1. One may easily see that $\widetilde{R}_{cr}$ decreases with $\widetilde{\Lambda}$, thus confirming the well-known destabilizing action of viscous dissipation (Barletta, Celli & Rees 2009*a*,*b*; Barletta & Nield 2010). Table 1 also reveals that a_{cr} is an increasing function of Λ. We note that, as $\widetilde{R}_{cr}$ decreases with $\widetilde{\Lambda}$, there exists a value $\widetilde{\Lambda} = 471.3847$ such that the onset of the instability occurs with $\widetilde{R}_{cr} = 0$. If $\widetilde{\Lambda} > 471.3847$, the basic flow becomes linearly unstable even with a negative $\widetilde{R}$. Physically, this means that the viscous dissipation, when $\widetilde{\Lambda} \geqslant 471.3847$, is so intense as to destabilize a porous layer with even boundary temperatures ($\widetilde{R} = 0$) or with a top boundary hotter than the bottom boundary ($\widetilde{R} < 0$). This special role played by the value $\widetilde{\Lambda} = 471.3847$ was previously revealed by Barletta, Celli & Rees (2009*a*) with reference to a horizontal porous layer ($\phi = 0$) having isothermal boundaries with the same temperature ($\Delta T = 0$).

The neutral stability curves $\widetilde{R}(a)$ are shown in figure 3 for different values of $\widetilde{\Lambda}$. One can notice that, when the value of $\widetilde{\Lambda}$ exceeds the threshold value $\widetilde{\Lambda} = 471.3847$, the minimum value $\widetilde{R}_{cr}$ of the parameter $\widetilde{R}$ becomes negative. The behaviour of $\widetilde{R}_{cr}$

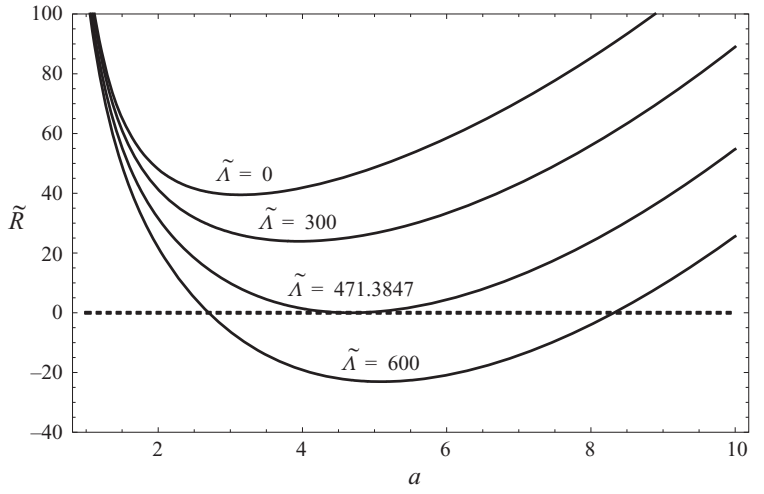

FIGURE 3. Longitudinal rolls: neutral stability curves, $\widetilde{R}(a)$, for different values of $\widetilde{\Lambda}$.

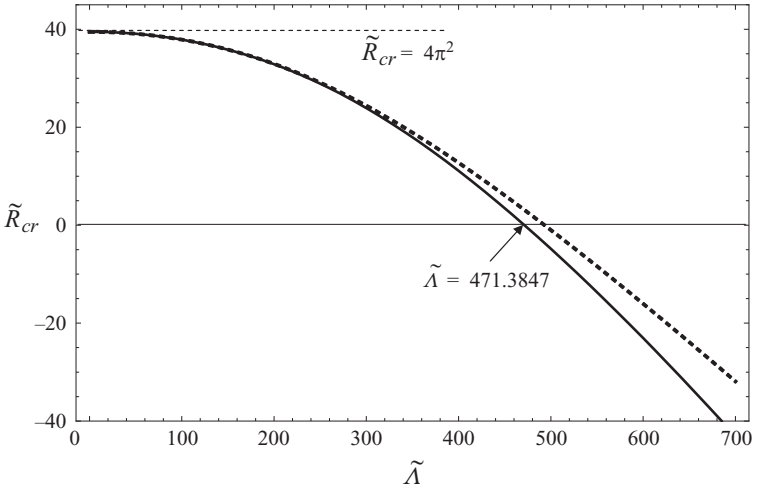

FIGURE 4. Longitudinal rolls: plot of $\widetilde{R}_{cr}$ versus $\widetilde{\Lambda}$. The solid line refers to the numerical solution and the dashed line refers to the weighted residual solution.

and a_{cr} versus $\widetilde{\Lambda}$ is also illustrated in figures 4 and 5. In these figures, the accurate numerical solution obtained by the Runge–Kutta method is compared with the $N = 2$ weighted residual solution. The latter solution loses precision as $\widetilde{\Lambda}$ increases, especially with respect to the evaluation of a_{cr} (figure 5).

The parametrization, based on $\widetilde{R}$ and $\widetilde{\Lambda}$, allows one to optimize the number of governing parameters, but it is not appropriate for illustrating the effect of the inclination angle on the onset conditions for the instability. Therefore, it is useful to see how an assigned pair (ϕ, Λ) determines the onset conditions (a_{cr}, R_{cr}). This task is easily accomplished by first solving (5.8), (5.9) and (5.11), and then by taking into account the definitions expressed by (5.10). Values of R_{cr} and a_{cr} are reported in tables 2 and 3, respectively. In these tables, different inclination angles ϕ are considered. Table 2 demonstrates that, on increasing the inclination of the layer

ϕ	$\Lambda = 0$	$\Lambda = 100$	$\Lambda = 200$	$\Lambda = 300$	$\Lambda = 400$
0°	$4\pi^2$	37.88950	32.86951	23.91902	11.09960
10°	40.08744	38.52333	33.58816	24.79179	12.16092
20°	42.01205	40.52143	35.83629	27.49804	15.44105
30°	45.58575	44.21459	39.93158	32.33934	21.26062
40°	51.53541	50.32538	46.57603	39.98193	30.29399
50°	61.41751	60.40472	57.29484	51.89103	43.96022
60°	78.95684	78.17088	75.77900	71.68295	65.73902
70°	115.4272	114.8906	113.2699	110.5325	106.6264
80°	227.3471	227.0751	226.2574	224.8897	222.9651

TABLE 2. Longitudinal rolls: values of R_{cr} versus Λ and ϕ.

ϕ	$\Lambda = 0$	$\Lambda = 100$	$\Lambda = 200$	$\Lambda = 300$	$\Lambda = 400$
0°	π	3.232423	3.516578	3.954144	4.399537
10°	π	3.229637	3.505127	3.932914	4.374292
20°	π	3.221629	3.472071	3.869984	4.297689
30°	π	3.209403	3.421288	3.768523	4.167702
40°	π	3.194483	3.359052	3.636622	3.984023
50°	π	3.178703	3.293317	3.489836	3.756351
60°	π	3.163971	3.232423	3.349803	3.516578
70°	π	3.152034	3.183666	3.237309	3.313954
80°	π	3.144279	3.152360	3.165896	3.184987

TABLE 3. Longitudinal rolls: values of a_{cr} versus Λ and ϕ.

above the horizontal, one obtains increasing values of R_{cr}. This qualitative behaviour of R_{cr} versus ϕ is perfectly compatible with that in the absence of viscous dissipation ($\Lambda = 0$). In the latter case, $R_{cr}\cos\phi$ is just given by $4\pi^2$ (Nield & Bejan 2006). On the other hand, $R_{cr}\cos\phi$ changes with ϕ when $\Lambda \neq 0$. Table 2 provides further interesting information. In fact, the critical wavenumber is π for every inclination angle if no viscous dissipation is present (Nield & Bejan 2006), whereas it changes with ϕ when $\Lambda \neq 0$. Due to the destabilizing effect of the viscous dissipation, R_{cr} decreases with Λ for every fixed angle ϕ. Hence, one may associate to every ϕ the corresponding value of Λ that yields the condition $R_{cr} = 0$. We pointed out above that $\widetilde{R}_{cr} = 0$ implies $\widetilde{\Lambda} = 471.3847$. In other words, from (5.10), $R_{cr} = 0$ is obtained when

$$\Lambda = \frac{471.3847}{\cos\phi}. \tag{5.19}$$

Obviously, the value of Λ expressed by (5.19) increases with ϕ and eventually tends to ∞ when the layer becomes vertical.

6. Transverse rolls

Assuming the disturbances to be y-independent, we have transverse rolls. The solutions of (4.2), (4.3), (4.5) and (4.7) are thus sought such that $V = 0$ and the fields U, W and θ depend only on (x, z, t). It is now convenient to introduce a streamfunction, ψ, such that (4.2) is satisfied,

$$U = \frac{\partial\psi}{\partial z}, \quad W = -\frac{\partial\psi}{\partial x}. \tag{6.1}$$

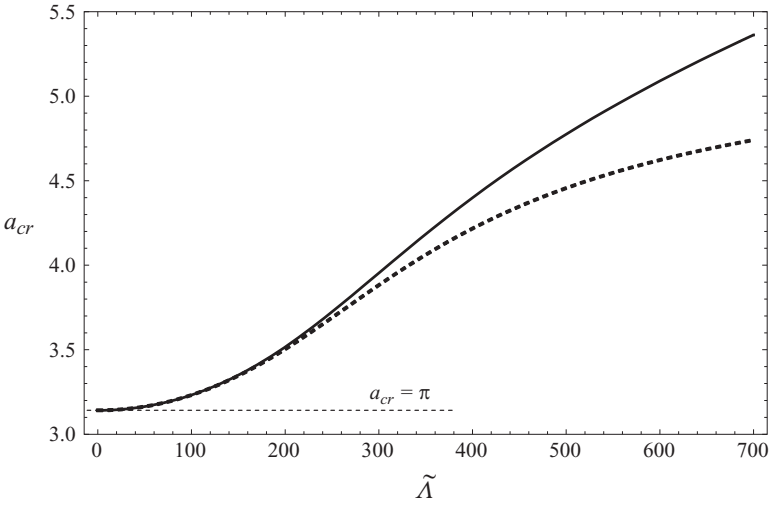

FIGURE 5. Longitudinal rolls: plot of a_{cr} versus $\widetilde{\Lambda}$. The solid line refers to the numerical solution and the dashed line refers to the weighted residual solution.

Equations (4.3) and (4.5) can thus be rewritten as

$$\nabla^2\psi = R\,\frac{\partial\theta}{\partial z}\,\sin\phi - R\,\frac{\partial\theta}{\partial x}\,\cos\phi, \tag{6.2}$$

$$\frac{\partial\theta}{\partial t} + u_B\,\frac{\partial\theta}{\partial x} - \frac{\partial\psi}{\partial x}\,G(z) = \nabla^2\theta. \tag{6.3}$$

The boundary conditions can be expressed as

$$z = 0, 1: \qquad \psi = \theta = 0. \tag{6.4}$$

An appropriate choice for the analysis of the neutral stability condition is seeking solutions of (6.2)–(6.3) in the form of plane waves,

$$\psi(x,z,t) = \mathrm{Re}\{\mathrm{i}\,f(z)\,\mathrm{e}^{\mathrm{i}(a\,x-\lambda\,t)}\}, \quad \theta(x,z,t) = \mathrm{Re}\{h(z)\,\mathrm{e}^{\mathrm{i}(a\,x-\lambda\,t)}\}, \tag{6.5}$$

where $\lambda = \lambda_R + \mathrm{i}\,\lambda_I$. As we are interested in the threshold condition of neutral stability, we now set $\lambda_I = 0$. Then substitution of (6.5) into (6.2)–(6.3) yields

$$f'' - a^2 f + \mathrm{i}\,R\,\sin\phi\,h' + a\,R\,\cos\phi\,h = 0, \tag{6.6}$$

$$h'' - \left[a^2 + \mathrm{i}\,a\,H(z)\,\tan\phi + \mathrm{i}\,\xi\right]h - a\,G(z)\,f = 0, \tag{6.7}$$

where

$$H(z) = \frac{u_B - Pe}{\tan\phi} = (1-z)\left(\widetilde{R} + z\,\frac{\widetilde{\Lambda}}{2}\right) - \frac{\widetilde{R}}{2}, \tag{6.8}$$

and $\xi = a\,Pe - \lambda_R$. By employing the definitions given in (5.7) and (5.10), (6.6) and (6.7) can be rewritten as

$$f'' - a^2 f + \mathrm{i}\,\tan\phi\,\widetilde{h}' + a\,\widetilde{h} = 0, \tag{6.9}$$

$$\widetilde{h}'' - \left[a^2 + \mathrm{i}\,a\,H(z)\,\tan\phi + \mathrm{i}\,\xi\right]\widetilde{h} - a\,\widetilde{G}(z)\,f = 0. \tag{6.10}$$

The boundary conditions can be expressed as

$$z = 0, 1: \qquad f = \widetilde{h} = 0. \tag{6.11}$$

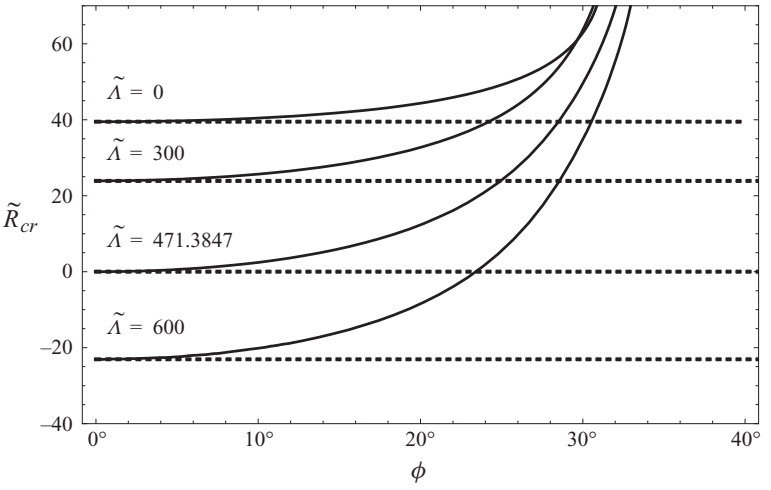

FIGURE 6. Plots of $\widetilde{R}_{cr}$ versus ϕ for longitudinal and for transverse rolls with different values of $\widetilde{\Lambda}$. The solid lines refer to transverse rolls and the dashed lines refer to longitudinal rolls.

The eigenvalue problem defined by (6.9)–(6.11) is again solved numerically by means of a sixth-order Runge–Kutta method coupled with the shooting method. The procedure is exactly the same as before for longitudinal rolls, except that here the eigenvalue problem is not self-adjoint so that the eigenfunctions $(f, \widetilde{h})$ are complex-valued. The results of the numerical solution are illustrated in figure 6. This figure shows the plots of $\widetilde{R}_{cr}$ versus ϕ for different values of $\widetilde{\Lambda}$. Both longitudinal and transverse rolls are considered. For the longitudinal rolls, there is a unique value of $\widetilde{R}_{cr}$ for a given $\widetilde{\Lambda}$, independent of the inclination angle ϕ (dashed lines in figure 6). On the other hand, for transverse rolls with a given $\widetilde{\Lambda}$, the parameter $\widetilde{R}_{cr}$ is an increasing function of ϕ (solid lines in figure 6). Figure 6 reveals that longitudinal and transverse rolls are equivalent for $\phi = 0$ but, as ϕ increases, $\widetilde{R}_{cr}$ for longitudinal rolls is always less than for transverse rolls. Therefore, as reasonably assumed in § 4, the longitudinal rolls are in every case more unstable than the transverse rolls. We note that the equivalence of the transverse and longitudinal rolls in the horizontal case ($\phi = 0$) can be interpreted as symmetry, relative to the onset of convection, between the x and y horizontal directions. This symmetry is broken when the porous layer is inclined above the horizontal, thus selecting the longitudinal rolls as the preferred mode of instability. This phenomenon can be traced back to the relationship between bifurcations and symmetry breaking pointed out by Golubitsky & Stewart (1985).

7. Conclusions

A basic parallel flow in an inclined porous channel has been studied, determined both by an imposed pressure gradient and by the buoyancy force. The buoyancy is due to the different temperatures assigned on the two boundary planes and to the effect of viscous dissipation. An approximate analytical solution of the local balance equations has been obtained under the realistic assumption that the Gebhart number, Ge, is very small. The governing dimensionless parameters are the Darcy–Rayleigh number, R, the viscous dissipation parameter, Λ, and the inclination angle, ϕ.

The linear response of the system to longitudinal roll disturbances has been investigated by adopting two solution methods: a second-order weighted residual solution,

an accurate numerical solution based on the sixth-order Runge–Kutta method and the shooting method. It has been shown that an appropriate parametrization of the eigenvalue problem, based on the modified parameters $\widetilde{R} = R\cos\phi$ and $\widetilde{\Lambda} = \Lambda\cos\phi$, allows one to encompass the dependence on the inclination angle ϕ. Instability arises when either R exceeds a critical value R_{cr}, for given Λ and ϕ, or $\widetilde{R}$ exceeds a critical value $\widetilde{R}_{cr}$, for a given $\widetilde{\Lambda}$. We have proved that R_{cr} is an increasing function of the inclination angle ϕ, for a prescribed Λ, and that R_{cr} is a decreasing function of Λ, for a prescribed ϕ.

The linear response of the system to transverse roll disturbances has also been investigated. In this case, the parametrization based on $\widetilde{R} = R\cos\phi$ and $\widetilde{\Lambda} = \Lambda\cos\phi$ does not allow one to reduce the number of governing parameters. This means that the critical value $\widetilde{R}_{cr}$ depends on ϕ, for every given $\widetilde{\Lambda}$. When $\phi = 0$ (horizontal channel), the value of $\widetilde{R}_{cr}$ coincides with that for longitudinal rolls. On the contrary, $\widetilde{R}_{cr}$ increases with ϕ for $\phi > 0$. This means that the transverse rolls are more stable than the longitudinal rolls. This result is expected on the basis of the behaviour, well known in the literature, for the limiting case of negligible viscous dissipation.

The investigation carried out in this paper demonstrated the role played by viscous dissipation as a possible source of convective instability. In particular, previous studies, published by these authors, focused on viscous dissipation as the sole cause of the instability. On the other hand, here viscous dissipation has been considered together with an externally imposed boundary temperature difference leading to the onset of convection. The subject of the dissipation-induced thermal instability leaves open several aspects that deserve attention and represent interesting opportunities for future research. Among these possible developments, we mention the nonlinear analysis of the instability that may provide new insight into the dynamics of the disturbance amplitudes, as well as on the prediction of the heat transfer rates at supercritical conditions.

REFERENCES

Abramowitz, M. & Stegun, I. A. 1965 *Handbook of Mathematical Functions*. Dover.

Barletta, A., Celli, M. & Nield, D. A. 2010 Unstably stratified Darcy flow with impressed horizontal temperature gradient, viscous dissipation and asymmetric thermal boundary conditions. *Intl J. Heat Mass Transfer* **53**, 1621–1627.

Barletta, A., Celli, M. & Rees, D. A. S. 2009*a* Darcy–Forchheimer flow with viscous dissipation in a horizontal porous layer: onset of convective instabilities. *ASME J. Heat Transfer* **131**, 072602.

Barletta, A., Celli, M. & Rees, D. A. S. 2009*b* The onset of convection in a porous layer induced by viscous dissipation: a linear stability analysis. *Intl J. Heat Mass Transfer* **52**, 337–344.

Barletta, A. & Nield, D. A. 2010 Instabilities of Hadley–Prats flow with viscous heating in a horizontal porous layer. *Trans. Porous Med.* **84**, 241–256.

Caltagirone, J. P. & Bories, S. 1986 Solutions and stability criteria of natural convective flow in an inclined porous layer. *J. Fluid Mech.* **155**, 267–287.

Cheng, K. C. & Wu, R. S. 1976 Viscous dissipation effects on convective instability and heat transfer in plane Poiseuille flow heated from below. *Appl. Sci. Res.* **32**, 327–346.

Eldabe, N. T. M., El-Sabbagh, M. F. & El-Sayed (Hajjaj), M. A. S. 2007 The stability of plane Couette flow of a power-law fluid with viscous heating. *Phys. Fluids* **19**, 094107.

Finlayson, B. A. 1972 *The Method of Weighted Residuals and Variational Principles*. Academic Press.

Golubitsky, M. & Stewart, I. 1985 Hopf bifurcation in the presence of symmetry. *Arch. Rat. Mech. Anal.* **87**, 107–165.

Ho, T. C., Denn, M. M. & Anshus, B. E. 1977 Stability of low Reynolds number flow with viscous heating. *Rheol. Acta* **16**, 61–68.

Johns, L. E. & Narayanan, R. 1997 Frictional heating in plane Couette flow. *Proc. R. Soc. Lond.* A **453**, 1653–1670.

Joseph, D. D. 1965 Stability of frictionally-heated flow. *Phys. Fluids* **8**, 2195–2200.

Nield, D. A. 2011 A note on convection patterns in an inclined porous layer. *Transp. Porous Med.* **86**, 23–25.

Nield, D. A. & Barletta, A. 2009 The Horton–Rogers–Lapwood problem revisited: the effect of pressure work. *Transp. Porous Med.* **77**, 143–158.

Nield, D. A. & Barletta, A. 2010 Extended Oberbeck–Boussinesq approximation study of convective instabilities in a porous layer with horizontal flow and bottom heating. *Intl J. Heat Mass Transfer* **53**, 577–585.

Nield, D. A. & Bejan, A. 2006 *Convection in Porous Media*, 3rd edn. Springer.

Nouar, C. & Frigaard, I. 2009 Stability of plane Couette–Poiseuille flow of shear-thinning fluid. *Phys. Fluids* **21**, 064104.

Rees, D. A. S. & Bassom, A. P. 2000 The onset of Darcy–Bénard convection in an inclined layer heated from below. *Acta Mechanica* **144**, 103–118.

Storesletten, L. & Barletta, A. 2009 Linear instability of mixed convection of cold water in a porous layer induced by viscous dissipation. *Intl J. Therm. Sci.* **48**, 655–664.

Subrahmaniam, N., Johns, L. E. & Narayanan, R. 2002 Stability of frictional heating in plane Couette flow at fixed power input. *Proc. R. Soc. Lond.* A **458**, 2561–2569.

Sukanek, P. C., Goldstein, C. A. & Laurence, R. L. 1973 The stability of plane Couette flow with viscous heating. *J. Fluid Mech.* **57**, 651–670.

Weber, J. E. 1975 Thermal convection in a tilted porous layer. *Intl J. Heat Mass Transfer* **18**, 474–475.

White, J. M. & Muller, S. J. 2002 Experimental studies on the stability of Newtonian Taylor–Couette flow in the presence of viscous heating. *J. Fluid Mech.* **462**, 133–159.

Wolfram, S. 2003 *The Mathematica Book*, 5th edn. Wolfram Media.

Yueh, C. S. & Weng, C. I. 1996 Linear stability analysis of plane Couette flow with viscous heating. *Phys. Fluids* **8**, 1802–1813.